Journal of Hazardous Materials 169 (2009) 195–202

Contents lists available at ScienceDirect

Journal of Hazardous Materials

journal homepage: www.elsevier.com/locate/jhazmat

An assembled poly-4-vinyl pyridine and cellulose triacetate membrane and Bi_2S_3 electrode for photoelectrochemical diffusion of metallic ions

Mourad Amara[a], Omar Arous[a,b], Fatima Smail[a], Hacène Kerdjoudj[a], Mohamed Trari[c], Aissa Bouguelia[c,*]

[a] Laboratory of Hydrometallurgy and Molecular Inorganic Chemistry Faculty of Chemistry, USTHB, BP 32, El Alia, 16111, Algiers, Algeria
[b] Centre of Research in Physical and Chemical Analysis CRAPC, PO BOX 248 Algiers RP 16004, Algiers, Algeria
[c] Laboratory of Storage and Valorization of Renewable Energies, Faculty of Chemistry, USTHB, BP 32, El Alia, 16111, Algiers, Algeria

ARTICLE INFO

Article history:
Received 16 November 2008
Received in revised form 16 March 2009
Accepted 18 March 2009
Available online 27 March 2009

Keywords:
Membrane selectivity
Poly-4-vinylpyridine
Ion transference
Bi_2S_3
Photoelectrochemistry
M^{n+} photodeposition

ABSTRACT

The transport phenomena across ion exchange membrane may be enhanced by applying various strengths inside or outside the system. The electrical current, generated by n-type semiconductor, is used to catalyse the separation of metal ions. The cation exchange membrane located between the two compartments allows both the separation and concentration of M^{n+} (Ag^+, Cu^{2+}, Pb^{2+} and Ni^{2+}). The flows of M^{n+} from the aqueous solution to—and inside the membrane are monitored by the determination of the fluxes and the potentials. In this study, the four cations are investigated alone or in quaternary systems. From photoelectrochemical measurement, the gap of Bi_2S_3 is found to be indirect at 1.65 eV. The shape of photocurrent potential curve and the negative flat band potential ($-1.02\ V_{SCE}$) give evidence of n-type character. The conduction band ($-1.25\ V_{SCE}$) yields thermodynamically M^{2+} photoreduction and catalyzes the diffusion process. The photoelectrode Bi_2S_3 makes the flux twofold greater than that observed in the dark. In all cases, the potential of the electrode M^{2+}/M in the feed compartment increases until a maximal value, reached at ~100 min above which it undergoes a diminution. The membrane is more selective to Cu^{2+} and this selectivity decreases in the quaternary system.

1. Introduction

Many works have been devoted to the separation and concentration of metal ions from different aqueous solutions. The membrane technologies and ion exchanges constitute in many cases the principal tools contributing to realize such studies. They have known a significant development during the last decades. Starting from the separation between ions [1,2], the membranes were developed by introducing new compounds or by modification of their surface yielding the separation between anions or cation with different valences [3–5]. Later, new generations of ion exchange membranes have been elaborated when the hydrophilic and hydrophobic balance is changed. These types of membranes allow the separation between ions of same valences [6]. Chelating agents are introduced in the functional groups of membrane permitting a specific behaviour toward a particular ion. The improvement of membrane for the separation process includes also the external parameters to the membrane like the electrical current density, the circulation flow in electrodialysis, the pressure in ultrafiltration, the pre-treatment in reverse osmosis as well as the composition of striping solution in Donnan dialysis. An attempt has been made to blend a solvent polymeric membrane formed by a polymer film containing a plasticizer. This liquid membrane acts either as facilitated carriers or chelating capture of ions since polyethyleneimine which forms complexes with some ions, especially copper ion and hexaoxa-diaza bicyclo hexacosane (2 2 2) cryptand as carriers [7]. This functional polymer membrane using supramolecular groups for recognition of ions or molecules has not in fact the real place as next alternative generation membrane.

On the other hand, a number of semiconductors have been used for the solar energy conversion [8–10]. A great deal of attention has been paid to metal sulfides owing to their technical applications like the hydrogen formation [11,12]. In a previous work, a commercial cation exchange membrane was used for the separation between nickel, copper and zinc ions in presence of the hexagonal wurtzite CdS as photoelectrode and which has the properties to be polarized when exposed to suitable light [13]. In the present work, photoactive Bi_2S_3 possesses interesting optical properties. It exhibits n-type conductivity and absorbs over the whole solar spectrum generating electron/hole (e^-/h^+) pairs which can eventuate in photoreactions in aqueous electrolytes. The electrons move through the external circuit to the counter electrode where they reduce the

* Corresponding author. Tel.: +213 21 24 79 50; fax: +213 21 24 80 08.
E-mail address: labosver@gmail.com (A. Bouguelia).

0304-3894/$ – see front matter © 2009 Elsevier B.V. All rights reserved.
doi:10.1016/j.jhazmat.2009.03.085

ions M^{2+}, after crossing the membrane, to elemental states and this constitutes the originality of the present work.

2. Experimental

2.1. Reagents

All the chemicals were from analytical reagent grade. The solutions of M^{n+} 0.1 mg/L and other reagents were prepared from salts (Merck): $AgNO_3$, $Ni(SO_4)7H_2O$, $Pb(NO_3)_2$, $Cu(SO_4)5H_2O$, $Bi_2(NO_3)_3$, KOH and HCl from Labosi whereas KI, KNO_3, cellulose triacetate, and poly-4-vinyl pyridine were purchased from Fluka. The solutions were diluted to the required volume with double distilled water. The electrode Bi_2S_3 and the new synthetic membrane formed by poly-4-vinyl pyridine and cellulose triacetate solvent polymeric method deals with our new approach. In this section, we describe the membrane preparation procedure, the electrode synthesis and the cell used for the metallic ions separation.

2.2. Membrane preparation

0.1 g of cellulose triacetate (CTA) and 0.1 g of poly-4-vinylpyridine were dissolved in 20 mL of chloroform. Then, 0.2 mL of tris-(2-ethylhexyl) phosphate (TEHP) is added under vigorous stirring during 4 h. The solution was transferred in a circular glass container and left for a slow evaporation during 24 h. The resulting membrane was extracted by addition of double distilled water and dried at 50 °C. The membrane CTA–TEHP–P4VP was characterized using chemical techniques as well as Fourier transform infra-red (FTIR). IR spectra were recorded on with Perkin–Elmer (Spectrum One) spectrophotometer. Ground sample was mixed with 200 mg of spectroscopically dry KBr and pressed into discs before the spectra were recorded.

2.3. Bi_2S_3 electrode preparation

A volume of 20 mL of NH_4OH was mixed to 180 mL of H_2O; the solution was agitated with a magnetic stirrer to get the first mixture. An adequate quantity of $Bi_2(NO_3)_3$ was then added under stirring and heated at 80 °C. Meanwhile, a second solution prepared by introduction of thiourea $SC(NH_2)_2$ and 50 mL of H_2O, was mixed carefully for 1 h, filtered and then washed with water. The final product is heat treated at 110 °C for 1 h, reground and retreated at 250 °C for a further 12 h. The black powder (Bi_2S_3) was soaked in acetic acid to remove preferentially Bi_2O_3 formed on the surface, washed with water and dried at 60 °C under reduced pressure. The discs (∅ = 13 mm and ~1 mm thickness) were made by pressing the powder under 2.5 kb, sintered in evacuated Pyrex tube at 500 °C during 4 h and then water quenched. The final product has been identified by X-ray diffraction using monochromatized Cu Kα radiation.

Copper wire was back contacted to the pellet with silver paste and encapsulated in a glass holder with epoxy resin. Electrochemical measurements were performed in a standard Pyrex-cell containing the working electrode (WE), a large-area Pt auxiliary electrode and a saturated calomel electrode (SCE) to which all potentials were scaled. The intensity–potential I (V) curves were plotted with to a potentiostat Voltalab PGP 301 under a nitrogen blanket. The capacitance of Bi_2S_3 was measured at a fixed frequency of 1.1 kHz. The electrode was brought near to the window to minimize the light absorption and to maintain a constant photon flux from run to run. The light source was a stabilized 200 W tungsten lamp (Osram) positioned obliquely with an angle of 45°. In that position, the flux intensity, measured with a digital radiometer (Testo 545) was found to be 35 mW cm^{-2}.

2.4. Analysis

A Cyber scan conductimeter (Sartorius Professional Meter PP-20) was used for the conductivity measurements. It also permits the determination of the potential in both compartments of the cell. Analysis of metal ions was carried out by using a PerkinElmer 2380 atomic absorption spectroscopy with the appropriate hallow cathode lamp for each element with corresponding wave length respectively 328.1 nm, 324.8 nm, 232 nm and 283.3 nm for Ag, Cu, Ni and Pb. The working flame is formed by air/acetylene gas. The concentration was deduced by interpolation from a calibration plot of adsorption versus M^{2+} concentration. Standard solutions of elements were freshly prepared just prior use. Silver was titrated by the Mohr method using NaCl as titrating salt and K_2CrO_4 as indicator. Nitrate was determined by a spectrometric method using sodium salicylate at 415 nm.

The diffuse reflectance spectrum was obtained on a Jasco V-500 spectrophotometer with MgO-coated integrating-sphere reflectance attachment.

2.5. Diffusion experiment

The diffusion of ions M^{n+} through the membrane was realized in unequal compartments cell described elsewhere [13] and composed by a strip compartment (50 mL) and a feed compartment (100 mL) designed with a Teflon material. The membrane after several cycles of pre-treatment was placed between the compartments. The volumes of the two compartments are maintained unequal in order to get a double concentration and to speed up the diffusion process of ions in the receipt compartment. n Bi_2S_3 electrode was introduced in the feed compartment containing 0.1 mg/L of M^{n+}.

3. Results and discussions

3.1. Characterization of Bi_2S_3 crystal structure

Bi_2S_3 was identified by X-ray diffraction. The pattern (Fig. 1) shows a single phase in agreement with the JCPDS card No 35-1401 and exhibits a medium crystallization. All the peaks are indexed in an orthorhombic unit cell with the lattice constants a = 11.181 nm, b = 11.393 nm and c = 4.028 nm. The specific surface area (1.3 m^2/g) was determined from the relation ($6/\rho_{ex}L$) where ρ_{ex} is the experimental density and L the crystallite size determined from the Scherrer formula. It is helpful to mention that when heating in air, Bi_2S_3 converts irreversibly to yellow Bi_2O_3. By contrast, when

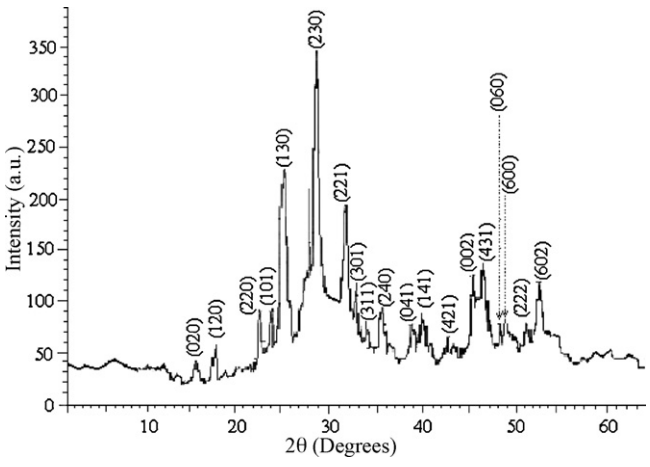

Fig. 1. X-ray diffraction of Bi_2S_3 compound.

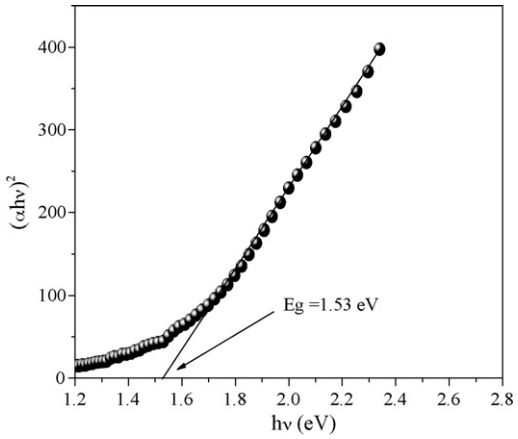

Fig. 2. Direct optical transition of Bi_2S_3.

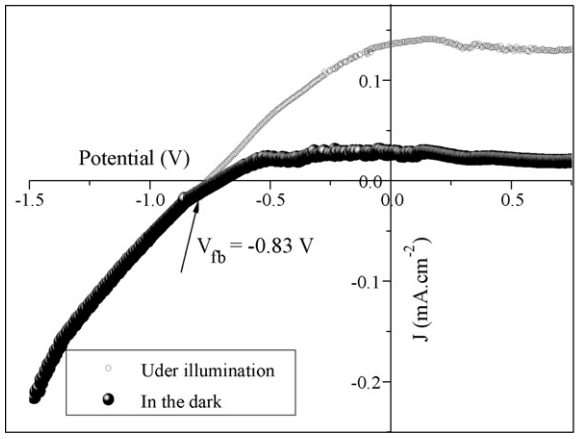

Fig. 3. The *I* (V) characteristics of Bi_2S_3 plotted in the dark and under illumination.

treated above 500 °C in evacuated tube, it decomposes to Bi and S as evidenced from XRD and optical microscopy. The choice of Bi_2S_3 as photocatalyst was determined by the low cost and an excellent chemical stability over the whole pH range.[1] It also proved its effectiveness as photocatalyst for hydrogen photoproduction [14]. In addition, the conduction band derives mainly from sulfur: 3p orbital with a lower electronegativity than the homologous oxygen: 2p orbital and therefore possesses a strong reducing power [15].

3.2. Optical properties and photoelectrochemistry

Bi_2S_3 is a direct band gap semiconductor; the optical absorption coefficient (α) depends on the incident energy ($h\nu$) [16]:

$$(h\nu\alpha)^2 = \text{Const}(h\nu - E_g) \quad (1)$$

The intercept of the linear plot $(h\nu\alpha)^2$ with the $h\nu$-axis yields E_g value of 1.53 eV (Fig. 2) in agreement with that previously reported [17] and the optical transition is directly allowed.

The photoelectrochemistry is based on the excitation of Bi_2S_3 by suitable light ($h\nu > E_g$). Bi_2S_3 indicates a rectifying junction at the electrolyte contact with a dark current (J_d) less than 3 mA cm^{-2} (Fig. 3). Below ~ -1 V, I_d increases owing to the water reduction. The photocurrent I_{ph} is an intrinsic property which appears when the electrode is polarized above the potential V_{fb}. I_{ph} increased progressively along the positive potential and beyond −0.7 V reaches a limiting value, a magnitude of which was found to depend only on the flux intensity. At potentials anodic of −0.9 V, it was masked by O_2-evolution.

[1] It does not dissolves only even for pH < 0 owing to the small solubility product ($K_s = 10^{-97}$).

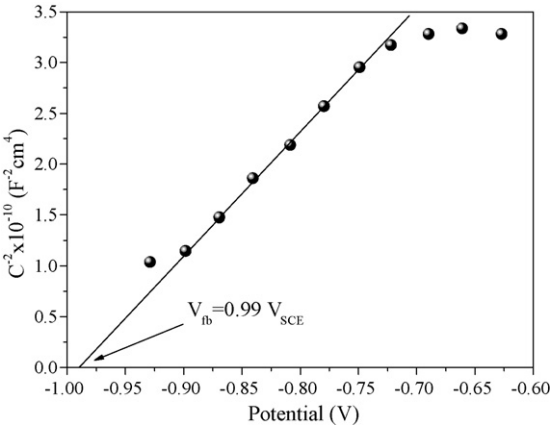

Fig. 4. The Mott Schottky characteristic of Bi_2S_3 in KOH solution.

The voltage at the interface required to preclude the lost of electron/hole (e^-/h^+) pairs by recombination varies to some extent with the material being considered. For zero recombination, a value of at least 0.3 V is needed. The junction electric field which takes place spontaneously permits the separation of photogenerated (e^-/h^+) pairs. The electrons in the conduction band (CB) move via the external circuit to reduce the ions M^{n+}. The potential V_{fb} has been

Table 1
Amounts of retained ions in the membrane bulk $[M^{n+}]_o = 10^{-2}$ M.

M^{n+} or A^-	Cl^- (KCl)	NO_3^- (KNO_3)	NO_3^- (HNO_3)	Cu^{2+}	Ni^{2+}
Retained amount (mmol/g)	0.60	0.76	9.92	7.62	9.82

Table 2
Peak values and the corresponding radicals in different membranes m(TAC) = 0.1 g, v(TEHP) = 0.2 mL.

Membrane	Peak value (cm^{-1})	Corresponding radical
CTA	3480–3550	O–H
	2935	C–H
	1755	C=O
	1526	COO^-
	1246	C–O–C asym
	1054	C–O–C sym
TEHP	2960	C–H
	1464	CH_2
	1381	CH_3
	1285	P=O
	1020	P–O–C
P4VP	2929	C–H
	1598	C=C
	1415	C=N
CTA-TEHP-P4VP	Same bonds and disappearance of four bands	
	1598	C=C (P4VP)
	1526	COO^- (CTA)
	1415	C=N (P4VP)
	1285	
	New bands	P=O (TEHP)
	803 and 701	Specific interactions between CTA, TEHP and P4VP

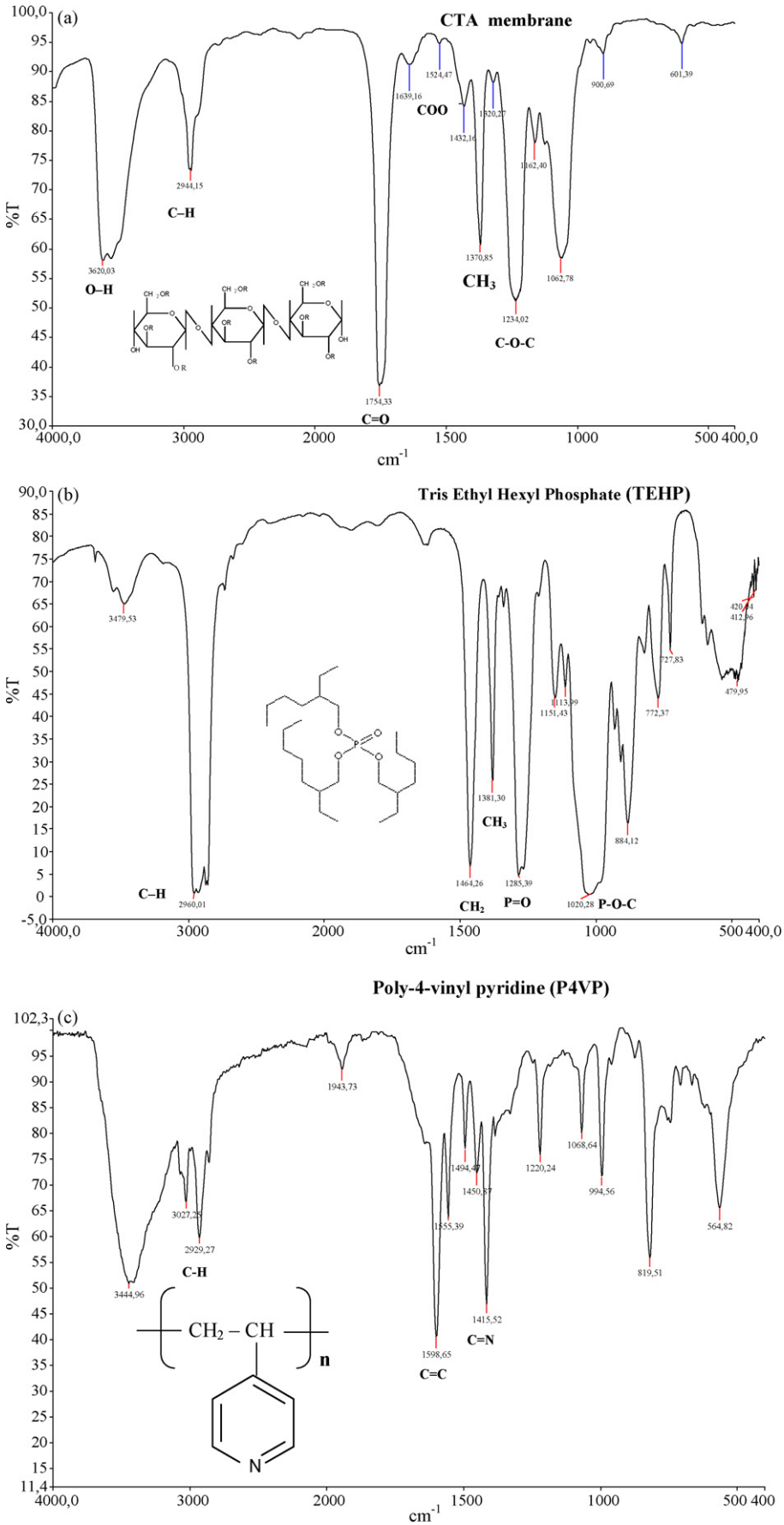

Fig. 5. (a) FTIR spectrum of cellulose triacetate membrane. (b) FTIR spectrum of Tris ethylhexyl phosphate (TEHP). (c) FTIR spectrum of poly-4-vinyl pyridine (P4VP). (d) FTIR spectrum of CTA + TEHP + P4VP membrane.

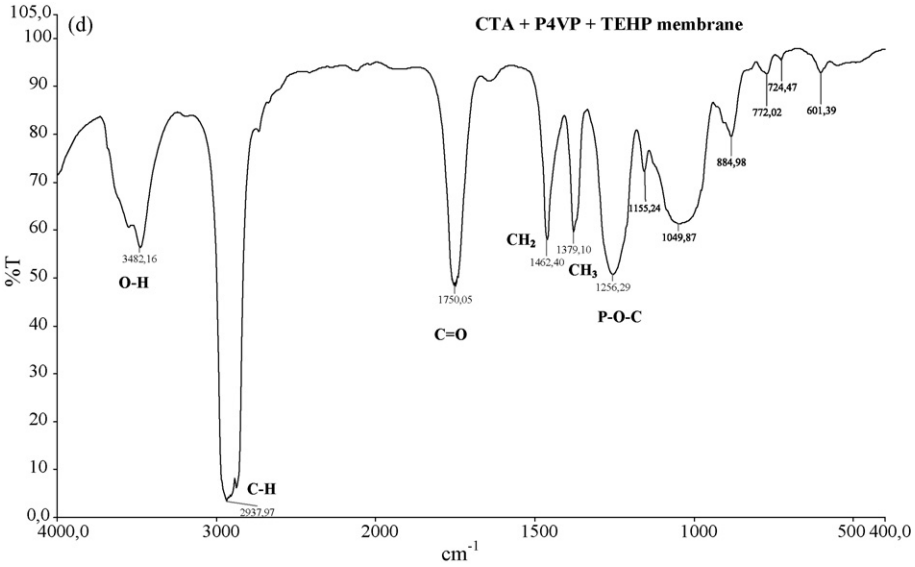

Fig. 5. (*Continued*).

accurately determined from the Mott Schottky plot:

$$\frac{1}{C_{SC}^2} = \frac{2}{e\varepsilon\varepsilon_0 A N_A}\left(V - V_{fb} - \frac{kT}{e}\right) \quad (2)$$

where A is the surface area and the symbols have their usual meaning. The potential V_{fb} (−0.43 V) and the electron density N_D (9.5×10^{15} cm^{-3}) were determined respectively from the extrapolation to $C^{-2} = 0$ and the slope of the plot (Fig. 4). The potential V_{fb} outlines the energetic position P of CB with respect to vacuum:

$$P = 4.75 + eV_{fb} - \Delta E \quad (3)$$

The P value of CB (4.18 eV/−0.57 V) is typical of materials in which CB is made up from S-3p orbital [18].

3.3. Characterization of membrane

The dried form of the membrane and the wet one (stirred in double distilled water for 24 h, then filtered-off by suction) are weighed, dried at 100 °C for 24 h and re-weighed; the obtained value was 9.2%. The quantities of metal ions adsorbed per unit mass of the synthetic membrane (mmol/g) were calculated using the following expression:

$$[M^{n+}]_{fixed}\,(mmol/cm^2) = ([M^{n+}]_0 - [M^{n+}]_{free})V/m;$$

m is the membrane weight, and V is the volume (mL). Table 1 gives the amounts of retained ion (NO_3^-, Cl^-, Cu^{2+} and Ni^{2+}) by the membrane. Such results confirm that the membrane synthesised by self-assembled polymer possesses an affinity to cations due to the external pyridine group. The high value of fixed nitrate anion in acidic medium might be explained by protonation of pyridium group which then returned to a positively groups capable to attract negatively charged species.

3.4. Infrared spectroscopy of membrane

Fig. 5a shows the spectrum of the cellulose triacetate membrane. The main features of this spectrum are an absorption band located around 1754 cm^{-1}, which is attributed to stretching vibrations of the carbonyl group. Bands at 1219 cm^{-1} and 1055 cm^{-1} correspond to the stretching modes of C–O single bonds. Less intense bands at 2944 cm^{-1} and 2880 cm^{-1} are attributed to C–H bonds and the wide band detected in the 3500–3100 cm^{-1} region is attributed to the O–H bonds stretching modes. Fig. 5b shows the spectrum of tris ethyl hexyl phosphate (TEHP). Bands at 1464 cm^{-1} correspond to the stretching modes of CH_2 bonds. Bands at 1381 cm^{-1} correspond to the stretching modes of CH_3 bonds. Bands at 1285 cm^{-1} and 1020 cm^{-1} correspond respectively to the stretching modes of P=O and P–O–C bonds. Fig. 5c shows the FTIR spectrum of P4VP. Bands at 1598 cm^{-1} correspond to the stretching modes of C=C bonds. Bands at 1415 cm^{-1} correspond to the stretching modes of C=N bonds. Table 2 collects the peak values and the corresponding radical of the reference CTA, TEHP, P4VP and CTA + TEHP + P4VP membrane.

The obtained results (Fig. 5d) show that all the maximum values extracted from the FTIR spectra of the CTA reference membrane, i.e. without TEHP and P4VP, are present in the modified membranes spectra. We observe the disappearance of four bands at 1598 cm^{-1} (stretching modes of C=C bonds) and at 1415 cm^{-1} (stretching modes of C=N bonds) of P4VP and at 1285 cm^{-1} correspond to the stretching modes of P=O bonds of TEHP. We also observe the appearance of two new bands centred at 803 cm^{-1} and 701 cm^{-1} putting in evidence specific interactions between CTA, TEHP and P4VP.

3.5. Diffusion phenomena

A combination of the membrane and Bi_2S_3 electrode has been used for the transport of metal ions as described elsewhere [13] in the cell schematised. The diffusion process has been followed by the measurement of the potential, the conductivity and the concentration in the feed compartment. Fig. 6a, b, c and d shows respectively the potentials of copper, silver, nickel and lead ions both in the dark and under illumination. The potential was measured in order to determine the diffusion equilibrium time and M^{n+} adsorption in the dark and under illumination. In both cases, it is observed a diminution of the global potential for copper solution using a specific electrode Cu^{2+}/Cu. The decrease of the potential indicates a migration of ions through the membrane from the feed compartment to the strip one.

For Ag^+, it is noticed a slight decrease in the potential when the experiment is carried out in the dark rather then in illumination conditions. Unlike other metal ions a sharp decrease of the potential in the case of transport of Ag^+ ions under illumination can also be assigned to the photochemical reduction of Ag^+ to Ag^0. Indeed, it

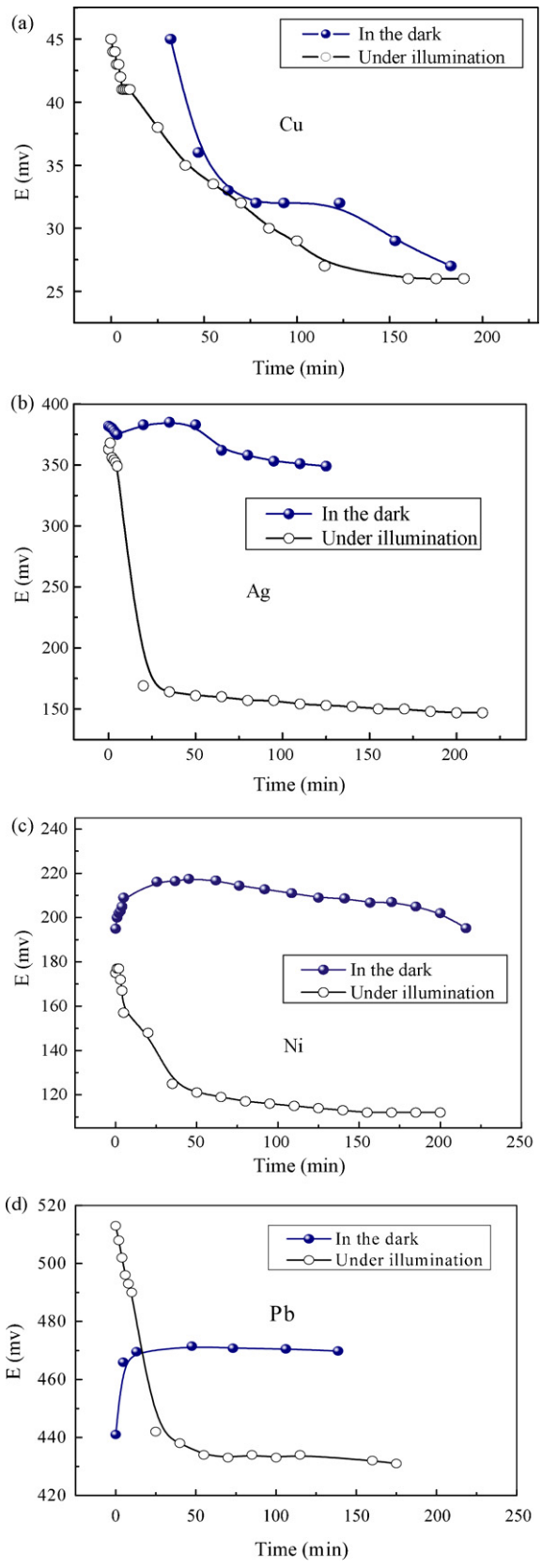

Fig. 6. (a) Variation of potential versus time of copper ion on the dark and under illumination. (b) Variation of potential versus time of silver ion on the dark and under illumination. (c) Variation of potential versus time of nickel ion on the dark and under illumination. (d) Variation of potential versus time of lead ion on the dark and under illumination.

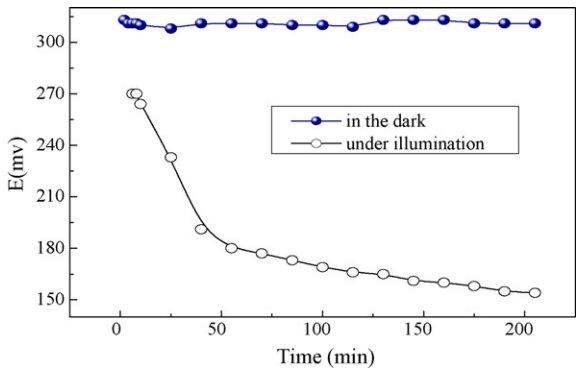

Fig. 7. Variation of potential value versus time of ions as a quaternary mixture on the dark and under illumination.

is well known that silver ions are easily reduced into metal under illumination.

A rapid stabilisation of the potential value is observed at ~20 min of experiment. This may be due to the great affinity of membrane to the monovalent ion. For Ni^{2+}, it is observed a slight increase of the potential in the dark and then a diminution to the initial value, which is attributed to the staying of nickel ion near the membrane surface in the feed compartment. By contrast, under illumination, the evolution of potential of Ni^{2+} has nearly the same shape as for silver.

For Pb^{2+}, the same variation is reported as in the case of nickel but with a more pronounced kinetic. After that, the competition between ions in the quaternary mixture system has been examined. Fig. 7 shows the variation of the potential for the four ions studied in the mixture with the same initial concentration as the alone metal. One can see that the illumination of Bi_2S_3 enhances the global migration of ions through the membrane, characterized by a decrease of the potential. Surprisingly, in the same period no evolution of the feed compartment was observed in the dark. These different variations suggest that the diffusion occurred as dialysis process without illumination, the membrane plays a role of separator between the solution and the migration owing to concentrations between the compartments. The electrodialysis process constitutes the system under illumination whose principal driven force is due to the electric field between the two compartments. These statements can be confirmed by the conductivity measurement in the feed compartment during the diffusion process whose main results are shown in Fig. 8.

At the beginning, the diffusion is characterized by a drastic increase of the potential in the dark, and then a stabilisation after ~10 min is observed. Under illumination of Bi_2S_3 electrode, a rapid decrease is observed, followed by an increase in 40 min. So, it may be concluded that the system represents a leakage on hydrogen

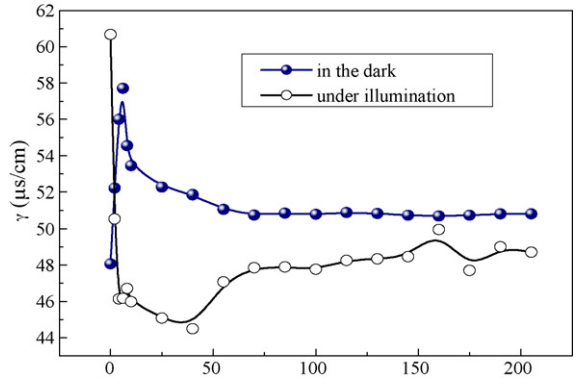

Fig. 8. Conductivity evolution in the feed compartment for the quaternary system.

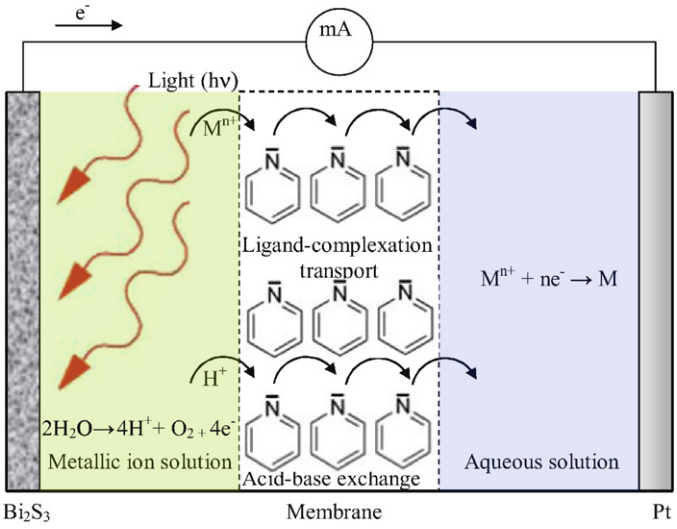

Fig. 9. A schematic representation of proton transference by acid/base exchange on the pyridine group and metal–ligand-complexation transport.

Table 3
The transference fluxes of metallic ions through the membrane in the dark and under illumination.

Flux × 10^{-9} (mol/s cm^2)	In the dark	Under illumination
$J_{Cu}{}^{2+}$	70	80
$J_{Pb}{}^{2+}$	69	73
$J_{Ni}{}^{2+}$	53	73
$J_{Ag}{}^{+}$	12	70

ion from the strip to the feed compartment. The proton leakage constitutes a general phenomenon concerning each type of cation exchange membrane. The hydrogen ions are provided by the water discharge on the illuminated cathode and then transported by membrane through an acid/base exchange between amino and ammonium groups of pyridine suspended on the membrane surface. A similar transference of proton has been previously suggested when commercial exchange membrane was modified by electro-adsorption of polyethyleneimine on the surface [19]. The proton leakage phenomenon is schematically represented in Fig. 9.

The kinetic of ions transfer using the flux calculation (Table 3) by the application of the equation: $J = \Delta n/(S\,\Delta t)$ shows that the system under illumination gives a rise to the transport of ions from the feed compartment to the strip one. The flux increase is more pronounced for Ag^+.

One of the most promising strategies for chemistry based solar energy conversion remains the semiconductor/liquid junction. When n-type Bi_2S_3 is immersed in aqueous solution, equilibrium is established by equalization of the electrochemical potentials resulting in an upward band bending B ($=E_{red}-V_{fb}$) of the electronic bands at the interface. The maximal photovoltage is imposed by the redox potential of the couple M^{n+}/M couple and the potential V_{fb} and in the ultimate case does not exceed ($\sim E_g$/e). The electrons move, through the junction electric field towards the counter electrode via the external circuit where they reduce the ion M^{n+} to the metal state. Indeed, the M^{2+} ions diffuse across the membrane to be photoelectrodeposited.

Bi_2S_3–CB is mainly formed from the orbital S^{2-}: 3p which provides a high energetic position. The potential of CB (−1.2 V) calculated from the relation $(4.75–V_{fb}+\Delta E)$[2] produces a large band bending in presence of M^{2+} permitting an efficient separation of the (e^-/h^+) pairs and a charge transfer between the Bi_2S_3–CB and the $M^{n+/0}$ couple followed by M^{2+} photoreduction:

$$Bi_2S_3 + h\nu \rightarrow h^+{}_{VB} + e^-{}_{CB} \quad (4)$$

$$2e^- + M^{2+} \rightarrow M_{\downarrow} \quad (5)$$

$$2H_2O + 2e^- \rightarrow H_2 + 2OH^- \quad (6)$$

The ions M^{n+}, after crossing the membrane, were reduced owing to their redox potentials of the couple M^{n+}/M appropriately located with respect to Bi_2S_3–CB. The electro-deposition catalyzes the diffusion process as proven by the ions transference flux J (Table 3) and the equilibrium (reaction (5)) strongly lies to the right hand, i.e. metal deposition. The observed saturation can be understood by the competitive hydrogen evolution. The metals are convenient for the water reduction as they are distinguished by small over potential. Once the metal M is deposited on Bi_2S_3, a bifunctional crystallite is formed and the H_2 liberation proceeds in a non-homogeneous fashion which affects the rate of the interfacial charge transfer and hence the global efficiency. The potential height is lowered and the electrons are channeled towards M catalytic sites where they reduce water.

4. Conclusion

The present work combined the solar energy with the environmental protection through the membrane selectivity for some metal ions. The study has permitted to show that the combination of many parameters deals to enhance separation and recuperation of metallic ions. The introduction of electrons in both sides of the synthetic membrane by illumination of Bi_2S_3 electrode constitutes an interesting approach. The pyridine group in the polymeric matrix of synthetic exchange membrane may be partially converted to pyridinium group and thus transference of proton provided from an anodic compartment by water dissociation is realized. The high kinetic and mobility of proton when transferred through membrane interface was observed by pH and conductivity variation during experiments. An important diffusion of metal ions was observed. This diffusion is obtained either as a simple migration from the both side of membrane by penetration in the pores and by jumping on the ammine group of pyridine. It has also been shown an increase of the diffusion flux when the electrode was activated by illumination. Bi_2S_3 has been elaborated through chemical route followed by heating in evacuated tube to preclude oxidation. Dark Bi_2S_3 absorbs over the whole solar spectrum. It has characterized structurally and photoelectrochemically. In addition, its low cost, exhibit long term stability and its flat band potential is suitably positioned to permit an efficient charge separation of the electron/hole pairs. The cations flow was considerably speeded up through the membrane with illuminated Bi_2S_3 electrode.

References

[1] F. Helfferich, Ion Exchange, McGraw Hill Inc., New York, 1962.
[2] Lakhshminarayanaiah, Transport Phenomena in Membranes, Academic Press, New York and London, 1969.
[3] T. Sata, R. Izuo, Y. Mizutani, R. Yamane, Transport properties of ion-exchange membranes in the presence of surface active agents, J. Colloid Interf. Sci. 40 (1972) 317–328.
[4] Y. Mizutani, Ion exchange membranes with preferential permselectivity for monovalent ions, J. Membr. Sci. 54 (1990) 233–257.
[5] M. Amara, H. Kerdjoudj, Modification of cation-exchange membrane properties by electro-adsorption of polyethyleneimine, Desalination 155 (2003) 79–87.
[6] M. Amara, H. Kerdjoudj, Electro-adsorption of polyethyleneimine on the anion exchange membrane: application to the nitrate removal from loaded solutions, Anal. Chim. Acta 547 (2005) 50–52.
[7] O. Arous, M. Amara, H. Kerdjoudj, Synthesis and characterization of cellulose triacetate and poly(ethylene imine) membranes containing a polyether macrobicyclic: their application to the separation of copper(II) and silver(I) ions, J. Appl. Polym. Sci. 93 (2004) 1401–1410.

[2] The activation energy ΔE (0.1 eV) was deduced from the conductivity measurements performed on sintered pellets.

[8] A. Derbal, S. Omeiri, A. Bouguelia, M. Trari, Characterization of new heterosystem $CuFeO_2/SnO_2$ application to visible-light induced hydrogen evolution, Int. J. Hydrogen Energy 33 (2008) 4274–4282.
[9] M. Younsi, S. Saadi, A. Bouguelia, A. Aider, M. Trari, Synthesis and characterization of oxygen-rich delafossite $CuYO_{2+x}$—application to H_2-photo production, Sol. Energy Mater. Sol. Cells 91 (2007) 1102–1109.
[10] S. Saadi, A. Bouguelia, A. Derbal, M. Trari, Hydrogen photoproduction over new catalyst $CuLaO_2$, J. Photochem. Photobiol. A 187 (2007) 97–104.
[11] R. Brahimi, Y. Bessekhouad, A. Bouguelia, M. Trari, Visible light induced hydrogen evolution over the heterosystem Bi_2S_3/TiO_2, Catal. Today 122 (2007) 62–65.
[12] R.M. Navarro, F. del Valle, J.L.G. Fierro, Photocatalytic hydrogen evolution from CdS–ZnO–CdO systems under visible light irradiation: effect of thermal treatment and presence of Pt and Ru cocatalysts, Int. J. Hydrogen Energy 33 (2008) 4265–4273.
[13] M. Amara, H. Kerdjoudj, A. Bouguelia, M. Trari, A combination between membrane selectivity and photoelectrochemistry to the separation of copper, zinc and nickel in aqueous solutions, J. Membr. Sci. 312 (2008) 125–131.
[14] Y. Bessekhouad, M. Mohammedi, M. Trari, Hydrogen photoproduction from hydrogen sulfide on Bi_2S_3 catalyst, Sol. Energy Mater. Sol. Cells 73 (2002) 339–350.
[15] David-R. Lide, Handbook of Chemistry and Physics, 78th edition, CRC Press, 1997–1998.
[16] I. Boldish Steven, William B. White, Optical band gaps of selected ternary sulfide minerals, Am. Mineral. 83 (1998) 865–871.
[17] P.S. Sonawane, L.A. Patil, Effect of nonstoichiometry on structural and optical properties of nanostructured Bi_2S_3 thin films prepared chemically at room temperature, Mater. Chem. Phys. 105 (2007) 157–161.
[18] X. Yu, C. Cao, H. Zhu, Synthesis and photoluminescence properties of Bi_2S_3 nanowires via surfactant micelle-template inducing reaction, Solid State Commun. 134 (2005) 239–243.
[19] M. Amara, H. Kerdjoudj, Modified membranes applied to metallic ion separation and mineral acid concentration by electrodialysis, Sep. Purif. Technol. 29 (2002) 79–87.